INFLUENCE OF CHEMICAL COMPOSITION AND STRUCTURE ON CHARACTERISTICS OF COLD RESISTANCE AND IMPACT STRENGTH OF LOW-CARBON STEEL

V. M. Goritskiy,[1] **G. R. Shneyderov,**[2] **and S. N. Vorob'ev**[3]

A method of ranking the work of ductile crack propagation (a_p) and critical brittleness temperature (T_{50}) was used to analyze the influence of ferrite grain size, pearlite and sulfide (sulfur) content, as well as hardness and concentration of phosphorus on the behavior and rate of T_{50} and a_p change.

The studies were carried out using the ductile-brittle transition criterion, according to which such transition is controlled by the size ratio of elementary microcracks of a brittle transcrystalline cleavage (Λ_b) and ductile (dimple) fracture (Λ_d). A correlation analysis procedure was used to study the influence of the grain size of ferrite, volumetric fraction of pearlite, amounts of sulfur and phosphorus, as well as the yield strength on the critical brittleness temperature (T_{50}). The same procedure was used to study the effect of sulfur content, pearlite volumetric fraction, as well as ferrite hardness (HV_{10}) and grain size on the work of ductile crack propagation in low-carbon steel. It was shown that the values of T_{50} and a_p are closely related to each other through the size of an elementary microcrack (dimple) during ductile fracture.

Keywords: low-carbon steel, critical brittleness temperature, work of ductile crack propagation, cold resistance, impact strength, sulfur content, pearlite content, ferrite grain size.

Introduction

The most important task of optimizing the chemical composition and structure of structural steels is to achieve a certain level of strength combined with an improved cold resistance and impact strength. The available literature sources [1–10] contain numerous data concerning the effect of sulfur (sulfide-type inclusions), titanium (nitride and oxide inclusions of various composition and morphology), and carbon (cementite and pearlite) on a complex of mechanical properties, including the critical brittleness temperature (T_{cr}) and impact strength. Until now, the explanation of the nature of cold brittleness (or ductile-brittle transition according to the terminology suggested in Ref. [11]) was based on the Cottrell–Petch equation [11, 12] presented in the following form:

$$\varepsilon T_{cr} = \sigma_0^* + C - \left(\frac{4q\mu\gamma'}{K_F - K_y} \right) d^{-1/2}, \tag{1}$$

where

[1] Melnikov Central Research and Design Institute of Steel Structures, Moscow, Russia; e-mail: goritskiyvit@bk.ru.

[2] Melnikov Central Research and Design Institute of Steel Structures, Moscow, Russia; e-mail: oem@stako.ru.

[3] Melnikov Central Research and Design Institute of Steel Structures, Moscow, Russia; e-mail: vsn-80@mail.ru.

σ_0^* is the temperature-independent component of friction stress in the Hall–Petch equation: $\sigma_t = \sigma_0 + K_y d^{-1/2}$;

γ' is the effective surface energy associated with crack growth;

μ is the shear modulus;

d is the grain size;

K_y is the coefficient characterizing the strength of dislocation blocking by impurity atoms;

q is the coefficient accounting for a degree of triaxiality of the stress condition;

K_F is the stress intensity coefficient (a constant in the following expression: $\sigma_F = \sigma_0 + K_F d^{-1/2}$ [1], which connects the breaking stress (σ_F) with the linear structural parameter (d));

C and ε are the constants.

As follows from Eq. (1), T_{cr} is a function of size d, a level of friction resistance of the lattice, and a portion of hydrostatic component in the applied stress.

A drawback of the Cottrell-Petch criterion is believed to be an obvious connection with only one parameter of the metal structure, i.e., the size of ferrite grain. Attempts made by a number of researchers to introduce the concept of an effective size of ferrite grain were unsuccessful. It is not clear what should be used as the distance (d_{eff}) between barriers that are opaque to sliding dislocations (according to V. I. Trefilov et al.[4]).

By using the approximation provided in Ref. [11, 12] and considering the unity of the micro-mechanisms of the beginning of brittle and ductile fracture, the authors of Ref. [13] suggested the following criterion of ductile-brittle transition:

$$T_{cr} = T_{cr}^* - \frac{B^* \sqrt{\Lambda_d}}{\Lambda_b},$$ (2)

where

Λ_d and Λ_b are the elementary dimensions of ductile (dimple) and brittle microcracks of transcrystalline cleavage, respectively;

$B^* = \alpha q \gamma' \mu / K_F \varepsilon$ (q is the stiffness ratio of the stress condition, which defines the tangent-to-normal stress ratio);

T_{cr}^* is the contribution to T_{cr} from the structural factors affecting the yield stress (yield point) of the ferritic matrix;

factor B^* accounts for the test conditions.

In general, the work of ductile crack propagation (a_p) can be presented as follows [14]:

$$a_p = \eta S_k \Lambda_d,$$ (3)

where S_k is the true breaking stress, and η is the proportionality factor, accounting for the test conditions, including the stress-strain behavior.

---

[4] V. I. Trefilov, Yu. Ya. Milman, and S. A. Firstov, *Physical Basics of Strength of Refractory Metals* [in Russian], Naukova Dumka, Kiev (1975).

It should be noted that the size of ductile dimple microcracks (dimples) is controlled by the size of carbide particles and non-metallic inclusions, which exceeds some critical value. In thermally improved steel 30Kh2NMFA, dimple formation is promoted by the particles of cementite (Fe_3C) and carbonitrides (V(C, N)) measuring $0.04\,\mu m$ and above [15]. Of special interest is the effect of the structural parameters on ferrite-pearlite steels, containing a significant amount of pearlite component. At the same time, it is not clear which structural and chemical factors control the level of cold brittleness and impact strength of the V-notch samples (Charpy). *The objective of the work* is to study the effect of the chemical composition and structural parameters on cold brittleness and work of ductile crack propagation in low-carbon steel sheet.

Materials and Procedure

The studies were performed using 25 smelting samples of St3sp sheet steel with a thickness of 6, 8, and 10 mm. The chemical composition of metal is characterized by a reduced content of nitrogen (0.005–0.007 wt.%) and non-ferrous metals, wt.%: Cr – 0.01–0.07, Ni – 0.02–0.06, and Cu – 0.04–0.08 (Table 1). Static tensile tests were performed on a universal TsD-40 tester using cylindrical type 3 samples according to GOST 1497-84. The impact strength (KCV) was determined using transverse samples (type 11 according to GOST 9454-78) at test temperatures ranging from $+20$ to $-60°C$ (three samples per test temperature). The work of ductile crack nucleation (a_n) and propagation (a_p) was calculated using the Neuhaus method based on the approaches described in Ref. [16].

Temperature T50 was used as the critical brittleness temperature, corresponding to the ductile-brittle transition, based on the presence of a 50% ductile component in the fracture of a V-notch impact sample. Steel structure was studied using etched longitudinal and transverse cross-sections by optical microscopy (Neofot-32) at a magnification $\times 200$ and $\times 500$. The size of ferrite grain was determined by a random linear intercept method (GOST 5639-82), while the degree of banding was assessed using points (GOST 5640-68). The Vickers hardness was determined using a TP-7R-1 instrument at a load of 98 N.

In order to determine the nature and degree of influence of the structural parameters and chemical elements on the characteristics of cold resistance and work of ductile crack propagation, the method proposed by V. M. Schastlivtsev et al. was used [17].

Results and Discussion

The studied steel samples had a ferritic-pearlitic structure. A typical structure steel with different carbon content is shown in Fig. 1. The structural characteristics, such as a volumetric fraction of pearlite, banding score, and nominal ferrite grain diameter, as well as hardness values of low-carbon steel samples are shown in Table 2. As can be seen from Fig. 2, despite a noticeable spread in experimental data, the T_{50} value is described by the Cottrell-Petch equation, when $T_{50} \approx \dfrac{1}{\sqrt{d}}$. In this case, the T_{50} values for sheet steel St3sp samples with thicknesses of 6, 8, and 10 mm can be satisfactory described by a general linear relationship.

In order to determine the nature of the structure and chemical elements and extent to which they affect the performance characteristics and mechanical properties of low-carbon steel St3sp, a method proposed by the authors of Ref. [17] was used. The reference numbers of the smelting samples will be kept the same as the ones shown in Table 1. Since the critical brittleness temperature (T_{50}) depends on the structural characteristics and chemical composition of steel, the whole set of experimental T_{50} values will be ranked in the order of monotonic change (decrease in cold resistance) of this characteristic. Then, while preserving the sequence in such

Table 1

Chemical Composition of the Studied Smelting Samples of Steel St3sp, wt.%

Smelting sample reference number	C	Si	Mn	S	P	Cr	Ni	Cu	N2
1	0.16	0.12	0.47	0.024	0.014	0.03	0.03	0.04	0.007
2*	0.16	0.21	0.51	0.020	0.013	0.04	0.04	0.06	0.006
3	0.15	0.20	0.49	0.022	0.012	0.03	0.03	0.04	0.005
4	0.18	0.21	0.45	0.006	0.012	0.03	0.04	0.06	0.006
5	0.14	0.16	0.45	0.020	0.012	0.02	0.02	0.02	0.005
6	0.18	0.20	0.43	0.011	0.013	0.04	0.03	0.08	0.006
7	0.15	0.22	0.48	0.019	0.011	0.04	0.04	0.06	0.005
8	0.20	0.20	0.43	0.014	0.013	0.03	0.02	0.07	0.007
9	0.18	0.20	0.43	0.011	0.013	0.04	0.03	0.08	0.006
10	0.15	0.22	0.48	0.019	0.011	0.04	0.04	0.06	0.005
11	0.15	0.22	0.48	0.019	0.011	0.04	0.04	0.06	0.005
12	0.16	0.22	0.45	0.020	0.017	0.03	0.03	0.08	0.006
13	0.18	0.20	0.46	0.013	0.014	0.03	0.02	0.04	0.007
14	0.17	0.21	0.45	0.017	0.021	0.04	0.03	0.05	0.006
15	0.18	0.20	0.46	0.013	0.014	0.03	0.02	0.04	0.007
16	0.15	0.18	0.46	0.016	0.009	0.01	0.02	0.04	0.007
17	0.16	0.20	0.45	0.013	0.009	0.03	0.03	0.05	0.005
18	0.17	0.21	0.45	0.017	0.021	0.04	0.03	0.05	0.006
19	0.15	0.22	0.48	0.019	0.011	0.04	0.04	0.06	0.005
20	0.19	0.22	0.45	0.016	0.017	0.05	0.03	0.05	0.005
21	0.16	0.17	0.40	0.014	0.011	0.03	0.03	0.07	0.007
22	0.19	0.25	0.46	0.033	0.017	0.07	0.06	0.06	0.005
23	0.17	0.23	0.51	0.018	0.018	0.04	0.03	0.05	0.005
24	0.16	0.17	0.40	0.014	0.011	0.03	0.03	0.07	0.007
25	0.16	0.19	0.45	0.022	0.015	0.03	0.03	0.04	0.005

Comments: * 0.01 wt.% As.

a variation series, the effect of structural factors and chemical element content on T_{50} will be analyzed (Fig. 3). As can be seen from Fig. 3(a), a number of characteristic areas can be identified on curve *1*, corresponding to samples Nos. 1–4, Nos. 6–9, and Nos. 22–23, which are characterized by a "steeper" rate of T_{50} increase, with some of these areas becoming plateaus, e.g., Nos. 4–6 and Nos. 9–11, respectively. It is worth pointing out that

Table 2
Structural Characteristics and Yield Strength of Steel

Smelting sample reference number	Critical brittleness temperature T_{50}, °C	Yield strength $\sigma_{0.2}$, MPa	Nominal diameter of ferrite graine* d, μm	Volumetric fraction* of pearlite F, %
1	−32	342	10.7 ± 0.5	15.4 ± 1.2
2	−40	307	10.3 ± 0.5	11.3 ± 1.1
3	−25	344	11.9 ± 0.6	10.4 ± 1.4
4	+23	280	14.1 ± 0.6	12.2 ± 1.0
5	−12	319	11.8 ± 0.5	14.1 ± 1.0
6	−16	353	11.2 ± 0.5	13.4 ± 1.6
7	−20	280	11.7 ± 0.5	13.3 ± 1.6
8	−19	283	11.4 ± 0.4	9.9 ± 1.9
9	0	316	14.4 ± 0.6	14.4 ± 1.8
10	−62	297	10.4 ± 0.4	8.0 ± 1.4
11	−45	270	10.5 ± 0.5	6.1 ± 1.5
12	7	285	14.1 ± 0.6	7.4 ± 1.8
13	5	297	13.4 ± 0.5	16.4 ± 1.3
14	9	338	16.4 ± 0.6	13.5 ± 2.0
15	−6	322	11.3 ± 0.5	10.8 ± 1.9
16	4	294	11.5 ± 0.4	8.0 ± 1.7
17	−2	310	13.8 ± 0.6	10.8 ± 1.0
18	22	245	16.0 ± 0.7	12.4 ± 0.9
19	−39	323	10.6 ± 0.4	10.5 ± 0.9
20	24	243	15.5 ± 0.5	16.2 ± 1.1
21	−39	379	10.5 ± 0.4	8.9 ± 1.4
22	−5	307	12.7 ± 0.5	11.5 ± 1.9
23	−19	331	11.0 ± 0.4	10.9 ± 2.0
24	−9	388	11.7 ± 0.5	22.0 ± 1.2
25	−52	314	8.5 ± 0.4	19.2 ± 1.3

Comments: * Note: mean values and standard deviation.

an extended gradual increase in T_{50} from sample No. 11 to sample No. 22 on the $T_{50} = f(N)$ line becomes more rapid in case of samples Nos. 23–24.

We will now analyze the effect of ferrite grain size (d) on T_{50}, which basically determines the position of the ductile-brittle transition according to Eq. (1). In general, despite several zigzags along the way, the $d = f(N)$
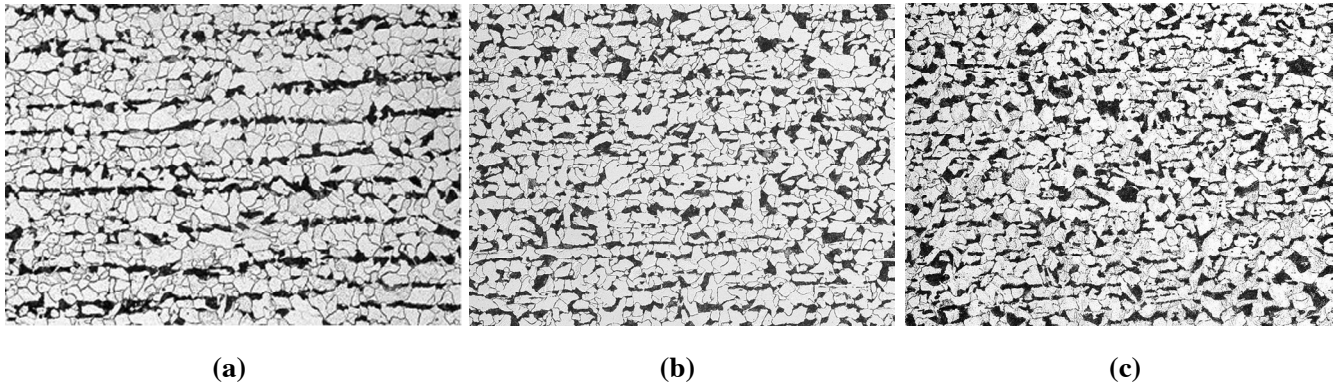
Fig. 1. Typical microstructure of steel St3sp containing 0.14% C (a), 0.15% C (b), and 0.19% C (c) with sheet thickness of 6 (a), 8 (b), and 10 mm (c).
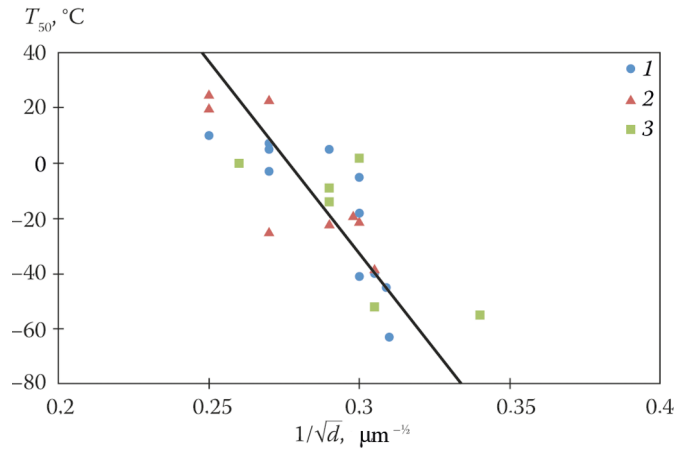

Fig. 2. Effect of the size (d) of ferrite grain on critical brittleness temperature (T_{50}) of low-carbon steel St3sp with sheet thickness of 6 (1), 8 (2), and 10 mm (3).
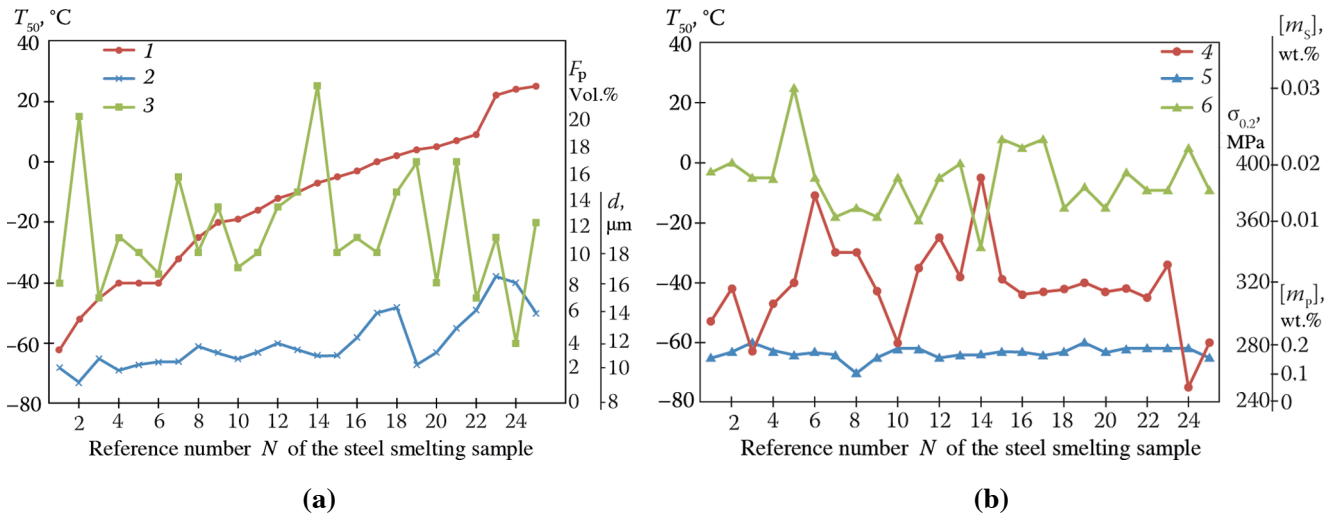

Fig. 3. Effect of the size (d) of ferrite grain (2), volumetric fraction of perlite (3), yield strength $(\sigma_{0.2})$ (4), sulfur content (5), and phosphorus content (6) on the variation series of an increase in critical brittleness temperature (T_{50}) (1) of steel St3sp.

graph demonstrates a tendency to increase, same as the $T_{50} = f(N)$ line (see Fig. 3). In the interval corresponding to samples Nos. 1–4, the nature of changes in the T_{50} and d values practically does not match. The rate of T_{50} increase from sample No. 1 to sample No. 4 is 6.25°C per 1 "step" in N. At the same time, the size of ferrite grain is practically the same and equal to $d = 10.3\ \mu m$. The rate of T_{50} increase from sample No. 6 to sample No. 9 is 6.6°C/step, which is almost the same as the rate of T_{50} increase for samples Nos. 1–4. In the interval corresponding to samples Nos. 1–4, there is a local "surge" of increased pearlite content (up to 19 vol. %) on the $F_p = f(N)$ line, and a small local increase (by 0.05 wt.%) in $[m_p]$ on the $[P] = f(N)$ line (see Fig. 3). At the same time, sample No. 2 is also characterized by a 0.01 wt.% content of arsenic, the effect of which is similar to that of phosphorus.

Thus, within an interval from sample No. 1 to sample No. 11, there are two sections (Nos. 1–4 and Nos. 6–11) with adjacent plateaus (Nos. 4–6 and Nos. 9–11), which demonstrate a sharp increase in T_{50} by a total of 45°C. The corresponding values of ferrite grain size on the $d = f(N)$ line are practically constant $(d = 10.3$–$10.5\ \mu m)$. Therefore, the sharp increase in T50 cannot be explained by the growing d-values. Hence, there should be other factors. Within the interval from sample No. 1 to sample No. 11, there is an increase in average pearlite content from 9 to 11 vol. %. Moreover, sharp increases in the fluctuation amplitude of F_p coincide with the areas of sharp increase in T_{50}. Plateau areas coincide with the minimum fluctuations of F_p (Fig. 3, line 3) and constant values of $[m_S]$ (Fig. 3(b)). In addition, the interval corresponding to samples Nos. 1–11 correlates with an interval of sharp increase in yield strength $(\sigma_{0.2})$ of steel (from 270 to 380 MPa) on the $\sigma_{0.2}$ line. According to Eq. (2), this is consistent with an increase in T_{cr}^{*}.

In the interval of gradual T_{50} increase from sample No. 11 to sample No. 23, the rate of T_{50} increase is 2.3°C/step. This interval correlates with the area of slight increase in the d-values from 11 to 11.8 μm (No. 11–No. 15), as well as wave-like increase in the d-values from 10.4 to 14.4 μm (No. 15–No. 19) and from 11.0 to 16.3 μm (No. 19–No. 23), while the values of $\sigma_{0.2}$ are decreasing. The latter decrease from 384 to 284 MPa, i.e., by 100 MPa. The interval corresponding to samples Nos. 22–23, which demonstrates a sharp (10°C/step) increase in T_{50}, correlates with a sharp decrease in F_p (from 13 to 4 vol. %) and a sharp decrease in $\sigma_{0.2}$ (from 338 to 243 MPa). Considering that within the interval corresponding to samples Nos. 22–23, the d-values showed an increase from 14 to 16 μm (i.e., a decreased contribution to T_{50}), while the value of $\sigma_{0.2}$ has decreased significantly (by 95 MPa), the growth of T_{50} must be caused by the pearlite component. At the same time, within the interval corresponding to samples Nos. 11–15, there is a sharp increase in $\sigma_{0.2}$, while within the interval from sample No. 15 to sample No. 23, an area of gradual reduction in $\sigma_{0.2}$ can be identified. Thus, a gradual increase in T_{50} within the interval from sample No. 15 to sample No. 23 is caused not only by the size of ferrite grain (d) and yield point of steel $(\sigma_{0.2})$, but also by pearlite (see Fig. 3). The F_p fluctuation range reaches 8–9 vol. %. A surprising fact can be seen in Fig. 3: although there is a sharp decrease in d-values (from 14.4 to 11 μm) within the interval corresponding to samples Nos. 18–19, this fact[5] is not reflected on the $T_{50} = f(N)$ line. An increase in $\sigma_{0.2}$ by 5 MPa can hardly explain this phenomenon. However, there is a distinct increase in $[m_P]$ from 0.18 to 0.20 wt.% observed on the $[P] = f(N)$ line. As follows from Fig. 2, the above-mentioned decrease in d according to the $T_{50} - \dfrac{1}{\sqrt{d}}$ line causes a drop in T_{50} by 27°C. For a low-carbon steel St3sp with ferrite + pearlite structure, a comparable effect of metal embrittlement can be expected as a result of phosphorus segregation along the grain boundaries, causing the development of intergranular brittleness, the percentage of which will constitute 15–18% [13].

It should be noted that the identified effect of pearlite on yield strength $(\sigma_{0.2})$ in low-carbon steel is consistent with the studies performed by Pickering and Gladman (1963). According to these studies, the embrittlement rate

---

[5] According to GOST 5639, this corresponds to a change in ferrite grain-size number from 9 to 10.

Table 3
Correlation and Coefficients of Linear Regression of the T_{50} Relationships
with the Studied Factors of Low-Carbon Steel

Factors	T_{50}	$[m_C]$	$[m_S]$	$[m_P]$	$\sigma_{0.2}$	d
T_{50}	1	0.2105	– 0.1041	– 0.0437	– 0.3508	0.8639
$[m_C]$	0.2105	1	– 0.2164	0.0852	– 0.2248	0.2112
$[m_S]$	– 0.1041	– 0.2164	1	0.0609	– 0.1136	– 0.126
$[m_P]$	– 0.0437	0.0852	– 0.0609	1	– 0.1514	– 0.0947
$\sigma_{0.2}$	– 0.3508	– 0.2248	– 0.1136	– 0.1514	1	– 0.3949
d	0.8639	0.2112	– 0.126	– 0.0947	– 0.3949	1
$b*$	– 148.82	45.191	14.083	22.44	0.00287	10.307

Comments: * b – coefficient of linear regression.

is 2.2°C/vol. % at $F_p > 5$ vol. %. Thus, the variation pattern of the $T_{50} = f(N)$ line over selected intervals depends not only on the size of ferrite grain (d), but also on other factors, including chemical, structural, and strength characteristics.

As can be seen from Table 3, this conclusion is confirmed by the results of linear correlation-regression analysis. The size of ferrite grain (d) is a major contributor to T_{50} change. The linear correlation coefficient of the $T_{50} – d$ relationship reaches $R = 0.864$, and the linear determination coefficient is $R^2 = 74.63\%$. In the second place in terms of the significance of its effect is $\sigma_{0.2}$: $R = – 0.351$ and $R^2 = 12.31\%$. In the third place in terms of the significance of its effect on T_{50} is pearlite $[m_C]$: $R = 0.211$ and $R^2 = 4.43\%$. To ensure equal assessment of the effect of chemical elements, the volumetric content of pearlite was replaced with carbon content expressed as a percentage. The effect of sulfur $[m_S]$ $(R = 0.104, R^2 = 0.11\%)$ and phosphorus $[m_P]$ $(R^2 = 0.02\%)$ on T_{50} is practically negligible. According to the results of linear multiple correlation analysis, the coefficient of multiple correlation of five mentioned elements with T_{50} reaches $R^* = 0.885$, and determination coefficient – $R^{*2} = 75.67\%$. The linear regression coefficient for the $T_{50} – [m_C]$ relationship reaches 45.191, while exceeding the b-value for the $T_{50} – d$ relationship by 4.5 times.

According to Ref. [13], such an increase in cold resistance of steels is caused by an earlier nucleation of large dimples in the vicinity of large pearlite colonies and sulfide inclusions according to Eq. (2). When analyzing ductile fractures, it was established that the dimple size (Λ_d) is related to the size of the pearlite colony face at the bottom of the dimple (L_p) by the following linear regression equation: $\Lambda_d = (3.8 \pm 1.8) + (1.32 \pm 1.38)L_p$ [13]. Such type of relationship between Λ_d and the size of sulfide inclusions was revealed in Ref. [13, 14]. Since in commercial steels, pearlite colonies and sulfide (oxysulfide) inclusions often have similar dimensions, the nucleation of dimples occurs along the front of a crack near a large-sized solid. The shape of such solid has a second-order effect [14]. For the studied steel smelting samples, containing from 0.009 to 0.021 wt.% P, no significant effect of the harmful impurity on T_{50} has been found (see Fig. 3, line 6).

The results of ranking the work of ductile crack propagation (a_p) are shown in Fig. 4. The choice of this impact strength component (KCV) is due to the fact that crack propagation is the factor that poses the greatest
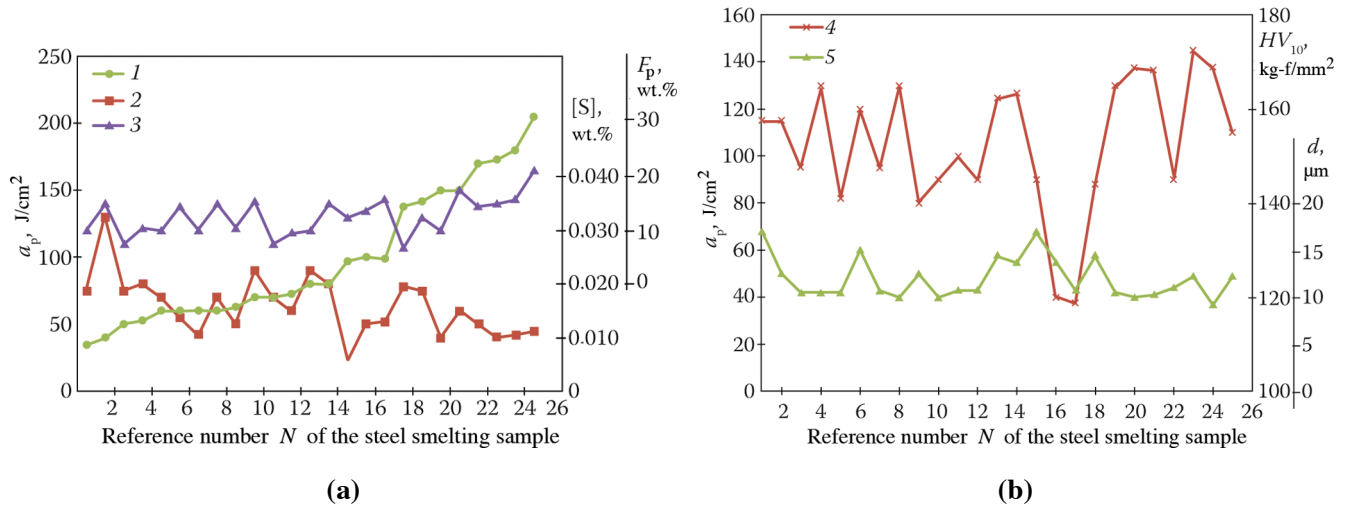
Fig. 4. Effect of sulfur content (*2*), volumetric fraction of perlite (*3*), hardness (HV_{10}) (*4*), and ferrite grain size (*5*) on the variation series of an increase in the work of ductile crack propagation (a_{p}) (*1*) of steel St3sp.

risk of brittle fracture of steel structures. An increase in the a_{p} value on the $a_{\mathrm{p}} = f(N)$ line within the interval from sample No. 1 to sample No. 5 coincides with an increase in average sulfur content in steel $[m_{\mathrm{S}}]$ (sulfide inclusions). Within the interval from sample No. 5 to sample No. 14, a moderate rate of a_{p} increase coincides with a sawtooth-shaped increase in the sulfur content in metal (see Fig. 4, line 2). The higher a_{p} increase rate (by ~ 2 times) within the interval from sample No. 14 to sample No. 25 corresponds to a decrease in the average sulfide content in steel (by ~ 1.4 times). Particularly impressive is a sharp increase in a_{p} within the interval from sample No. 22 to sample No. 25, which corresponds to a significant decrease (by 1.6 times) in the amount of sulfide inclusions at a moderate content of pearlite (see Fig. 4, line 3).

By considering a combined effect of sulfides and pearlite, it becomes possible to explain a sharper and approximately a twofold increase in the growth rate of the $a_{\mathrm{p}} = f(N)$ line, starting from sample No. 17 to sample No. 25. A similar situation was previously described in Ref. [14]. At a moderate pearlite content in steel and decreased amount of sulfide inclusions, the Λ_{d} value increases, since a dimple near large-sized sulfides has enough time to grow to a relatively large size. As the sulfur content $[m_{\mathrm{S}}]$ grows, the number of large dimples (Λ_{d}) increases, and they begin to merge, causing the T_{cr} value to decrease. Upon reaching some critical value $([m_{\mathrm{S}}] = [m_{\mathrm{S}}^{\mathrm{cr}}])$, the Λ_{d} sizes decrease, as the large dimples collide with each other, thereby limiting and then decreasing their size. The value of $[m_{\mathrm{S}}^{\mathrm{cr}}]$ depends on the amount of pearlite and other non-metallic inclusions, since, as large solids, they initiate large dimples. As a result, the T_{cr} value increases in the range of $[m_{\mathrm{S}}] > [m_{\mathrm{S}}^{\mathrm{cr}}]$. According to Ref. [14], such characteristic impact of Λ_{d} on T_{cr} explains the "sulfide effect" phenomenon. The latter consists in the fact that an increase in $[m_{\mathrm{S}}]$ in deoxidized steel leads to a decrease in impact strength during ductile fracture, while the critical brittleness temperature, paradoxical as it may sound, shifts toward the region of lower temperatures. This effect was discovered for the first time by the authors of Ref. [18]. The shift reaches 30–60°C [19].

As can be seen from Fig. 4, line 3, the curve of pearlite distribution in steel mostly has a saw-tooth shape. Some distortion of the shape of the $F_{\mathrm{p}} = f(N)$ line is observed within the interval from sample No. 10 to sample No. 17, when the lower "half-wave" includes intervals Nos. 11–14 and Nos. 14–17, consisting of three and two N-chains. This local deviation from the proper saw-tooth shape of the $F_{\mathrm{p}} = f(N)$ line coincides with

Table 4
Correlation and Coefficients of Linear Regression of the a_p Relationships
with the Studied Factors of Low-Carbon Steel

Factors	a_p	[S]	F_p	HV_{10}	d
a_p	1	-0.3258	0.4222	0.138	-0.2176
[S]	-0.3258	1	-0.0574	0.256	-0.0681
F_p	0.4222	-0.0574	1	-0.1145	-0.218
HV_{10}	0.138	-0.256	-0.1145	1	-0.131
d	-0.2176	-0.0681	-0.218	-0.131	1
b^*	-13.266	-3545.3	4.9076	0.9574	-2.9249

Comments: $* b$ – coefficient of linear regression.

the local sharp changes in the shape of $a_p = f(N)$ (steep segments and plateaus). A sharp increase in a_p over the interval from sample No. 18 to sample No. 25 is accompanied by a distinct decrease in the average pearlite content over the interval from sample No. 18 to sample No. 20. This pearlite content later increases from No. 21 to No. 23, but at the same time, the sulfur content ($[m_S]$) on the $F_p = f(N)$ line decreases within the interval from sample No. 21 to sample No. 25. The size of the dimple, formed near the pearlite colony, increases accordingly. Thus, comparably-sized sulfide inclusions and pearlite colonies behave almost equally in terms of their influence on the formation of large dimples around large-sized solids. According to Eq. (2), larger dimples are associated with higher cold resistance and greater a_p values.

Except for the interval Nos. 16–17 on the $HV_{10} = f(N)$ line, there is no significant effect of hardness (HV_{10}) (strength) of steel on the a_p values (see Fig. 4). Within the interval from sample No. 16 to sample No. 17, a distinct minimum ($HV_{10} = 119–121$ kg-f/mm^2) is identified, which corresponds to a plateau on the $a_p = f(N)$ line. A subsequent sharp jump in the HV_{10} values up to $168–172$ kg-f/mm^2 at a decreased contribution of pearlite and sulfides indicates a noticeable effect of HV_{10} on a_p. However, such effect only takes place when there is a sharp (by ~ 50 kg-f/mm^2) increase in hardness. By comparing the nature of variation of the size of ferrite grain (see Fig. 4, line 5), when d fluctuates in the range of 8.5–15.5 μm, no noticeable effect of the size of ferrite grain on the a_p value can be established.

Table 4 shows the results of linear correlation analysis of the relationship between a_p and the following factors: sulfur content $[m_S]$, volumetric pearlite fraction (F_p), hardness (HV_{10}), and ferrite grain size. As can be seen, the volumetric pearlite fraction has the greatest effect on the a_p value (linear correlation coefficient – $R = 0.422$; determination coefficient – $R^2 = 17.82\%$). Sulfur content is in the second place in terms of its effect on a_p ($R = -0.326$ and $R^2 = 10.61\%$), causing a reduction of the a_p value. This confirms the fact that the abundance of large-sized initiators of dimple nucleation combined with an increase in the amount of sulfides leads to the collision of dimples with each other, thus resulting in a decrease in the dimple size, and hence, a_p values. The latter are practically not impacted by the size (d) of ferrite grain ($R = 0.218$, $R^2 = 4.73\%$) and hardness (HV_{10}) ($R = 0.138$, $R^2 = 1.90\%$).
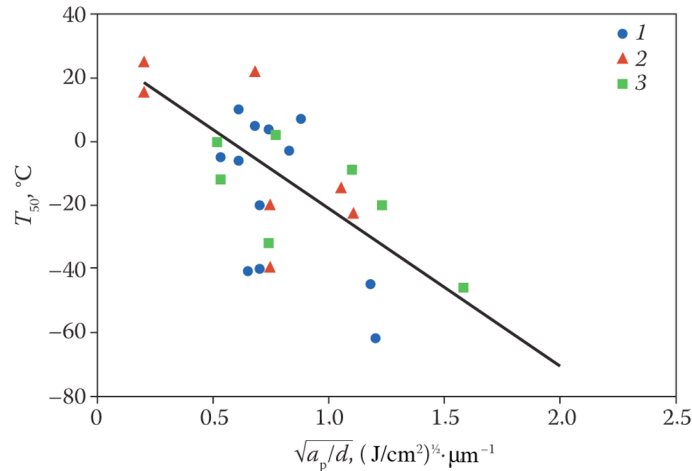
Fig. 5. Relationship between the critical brittleness temperature (T_{50}) and $\sqrt{(a_\text{p})/d}$ ratio for sheet steel St3sp with a thickness of 6 (*1*), 8 (*2*), and 10 mm (*3*).

It is important to note a very high value of the linear regression coefficient for sulfide inclusions, which reaches $b = -3{,}545.3$. It is due to the effect of pearlite and sulfides that the multiple correlation and determination coefficients reach the following values: $R^* = 0.598$ and $R^{*2} = 35.71\%$, respectively.

By comparing Eq. (2) and (3), the following expression can be derived:

$$T_\text{cr} = T_\text{cr}^* - \frac{B\sqrt{a_\text{p}}}{\sqrt{\eta S_k \Lambda_\text{b}}}. \tag{4}$$

As can be seen from this expression, when maintaining the test conditions, the following can be expected: $T_\text{cr} \sim -\dfrac{\sqrt{a_\text{p}}}{\sqrt{\eta S_k \Lambda_\text{b}}}$. For steels with ferritic and ferritic-pearlitic structure (when $\Lambda_\text{b} = d$), the following can be obtained: $T_\text{cr} \sim -\dfrac{\sqrt{a_\text{p}}}{\sqrt{S_k d}}$, which can be approximated by $T_\text{cr} \sim -\dfrac{\sqrt{a_\text{p}}}{d}$.

The correlation between the critical brittleness temperature $(T_\text{cr} = T_{50})$ and $\dfrac{\sqrt{a_\text{p}}}{d}$ is shown in Fig. 5.

In this case, the linear correlation coefficient of the $(T_{50} -\!\!- \dfrac{\sqrt{a_\text{p}}}{d})$ relationship is $R = -0.777$, and the linear determination coefficient is 60.37%. For comparison purposes, the linear correlation coefficient for the $(T_{50} - a_\text{p})$ relationship is $R = -0.188$, and the linear determination coefficient is $R^2 = 3.53\%$. Thus, there is a physico-mechanical link between the cold resistance parameter (T_{50}) and work of ductile crack propagation (a_p), as a component of impact strength (KCV).

CONCLUSIONS

1. A method of ranking the values of the critical brittleness temperature (T_{50}) was used to show that within certain sections of the $T_{50} = f(N)$ relationship, the rate of T_{50} increase does not always coincide with

an increase in the size (d) of ferrite grain, as follows from the Cottrell–Petch equation, however, it is definitely related to the content of pearlite (carbon) and the value of yield strength $(\sigma_{0.2})$ in low-carbon steel. There was no noticeable effect of phosphorus in the amount of 0.006–0.024 wt.% and sulfides (oxysulfides) on steel St3sp embrittlement.

2. A method of ranking the work of ductile crack propagation (a_p) was used to establish the following: (a) a moderate increase in a_p within the interval from sample No. 1 to sample No. 6 is caused by a decrease in sulfur content ranging from 0.033 to 0.006 wt.%; (b) a gradual growth of a_p in steel within the interval from sample No. 8 to sample No. 14 coincides with a sawtooth-shaped increase in the average sulfur and pearlite content; (c) a sharp increase in a_p (by ~ 2 times) within the interval from sample No. 14 to sample No. 25 corresponds to a decrease in sulfur (sulfides) content in steel from 0.020 to 0.006 wt.% with an increase in pearlite content in the range from 7.5 to 22 vol. %; (d) no significant effect on a_p of the size (d) of ferrite grain and hardness of steel (HV_{10}) was established, except for the interval from sample No. 17 to sample No. 25.

3. According to the results of correlation-regression analysis, the following has been established: the critical brittleness temperature (T_{50}) of low-carbon steel mainly depends on the size of ferrite grain (linear correlation coefficient – $R = 0.864$, linear determination coefficient – $R^2 = 74.63\%$), and also depends on the yield strength $(\sigma_{0.2})$ $(R = -0.351, R^2 = 12.31\%)$, while weakly depending on the content of carbon (pearlite) $(R = 0.211, R^2 = 4.43\%)$ and being independent of the content of sulfur (0.006–0.022 wt.%) and phosphorus (0.009–0.021 wt.%).

4. According to the results of correlation-regression analysis, the work of ductile crack propagation (a_p) depends on the volumetric fraction of pearlite (carbon) $(R = 0.422, R^2 = 17.82\%)$, sulfur (sulfides) $(R = -0.326, R^2 = 10.61\%)$, and is practically independent of the size of ferrite grain $(R = -0.218, R^2 = 4.73\%)$ and hardness (HV_{10}) $(R = 0.138, R^2 = 1.90\%)$. For the $(a_p - [m_S])$ relationship, the linear regression coefficient $(b = -3,545.3)$ is two orders of magnitude greater than that of the $(a_p - F_p)$ relationship $(b = 4.91)$.

5. By using a generalized criterion of ductile-brittle transition, according to which the latter is controlled by a size ratio of the elemental microcracks of brittle trans-crystalline cleavage (Λ_b) and ductile dimple fracture (Λ_d), it is shown that the values of T_{50} and a_p are linked by the following correlation:

REFERENCES

1. P. D. Odesskii, "Potential requirements for steels used in metal structures," *Deformatsiya i Razrusheniye Materialov*, No. 7, 67–74 (2005).
2. L. I. Gladshteyn, N. P. Larionova, and B. F. Belyaev, "Effect of ferritic-pearlitic microstructure on the properties of structural steels," *Metallurg*, No. 8, 45–53 (2012).
3. V. N. Skorokhodov, P. D. Odesskii, and A. V. Rudchenko, *Construction Steel* [in Russian], Metallizdat, Moscow (2002).
4. W. F. Spitzig, "Effect of sulfide inclusion morphology and pearlite banding on mechanical properties in normalized C–Mn steels," *Metal. Trans. A.*, **14A**(2), 271–283 (1983).
5. A. G. Glebov, M. A. Shtremel, and K. L. Kosyrev, "Areas of impurity effect on impact strength of thick steel plate," *Stal'*, No. 5, 95–97 (2004).
6. L. I. Efron, Yu. D. Morozov, and Ye. A. Goli-Oglu, "Effect of controlled rolling conditions on structure refinement and a complex of mechanical properties of low-carbon micro-alloyed steels," *Stal'*, No. 5, 67–72 (2011).
7. Ye. A. Goli-Oglu, L. I. Efron, and Yu. D. Morozov, "Improvement in the efficiency of thermomechanical treatment of micro-alloyed steels," *Stal'*, No. 2, 52–57 (2013).
8. L. I. Efron, *Science of Metals in Iron and Steel Making* [in Russian], Metallurgiya, Moscow (2012).
9. G. A. Artikov, V. F. Belyaev, and L. I. Gladshteyn, "Effect of cold molding on the mechanical properties of closed bent-welded profiles," *Promyshlennoye i Grazhdanskoye Stroitel'stvo*, No. 5, 16–18 (1994).

10. Yu. I. Morozov, M. Yu. Matrosov, S. Yu. Nastich, and A. B. Arabey, "New generation of high-strength pipe steels with a ferrite-bainite structure," *Metallurg*, No. 8, 39–42 (2008).

11. N. J. Petch, "The ductile-brittle transition in the fracture of α-iron," in: *The Atomic Mechanism of Fracture* (Transl. from English), Metallurgiya, Moscow (1963).

12. A. H. Cottrell, "Theoretical aspects of the fracture process," in: *The Atomic Mechanism of Fracture* (Transl. from English), Metallurgiya, Moscow (1963).

13. V. M. Goritskii, *Thermal Brittleness of Steels* [in Russian], Metallurgizdat, Moscow (2007).

14. V. M. Goritskii, *Application of Impact Strength Characteristics in Engineering Practice* [in Russian]. Metallizdat, Moscow (2016).

15. V. M. Goritskii and I. A. Guseva, The relationship between the dimple fracture parameters and structural characteristics of thermally-enhanced steel," *Fizika Metallov i Metallovedeniye (FMM)*, **56**, No. 1, 192–194 (1983).

16. V. M. Goritskii and D. P. Khromov, "Assessment of crack propagation resistance based on the impact strength test results," *Zavodskaya Laboratoriya*, No. 7, 70–72 (1984).

17. V. M. Schastlivtsev, I. L. Yakovleva, N. A. Tereshchenko, V. V. Kurban, et al., "Specifics of chemical composition and structure of low-carbon low-alloy steels after controlled rolling," *Metallovedeniye i Termichaskaya Obrabotka Metallov (MiTOM)*, No. 5 (635), 3–8 (2008).

18. B. H. Kapadia, A. T. English, and W. A. Backofen, "Influence of mechanical fibering on brittle fracture in hot rolled steel plate," *Trans. ASM*, **55**, 389–410 (1962).

19. Ye. N. Zhukova and N. M. Fonshteyn, "Effect of sulfur on the resistance of low-alloy steels to brittle fracture," *Stal'*, No. 5, 66–70 (1981).